

Image Reconstruction Method for Dual-energy Computed Tomography

Wenxiang Cong, Daniel Harrison, Yan Xi, Ge Wang

Abstract—Dual-energy computed tomography (CT) is to reconstruct images of an object from two projection datasets generated from two distinct x-ray source energy spectra. It can provide more accurate attenuation quantification than conventional CT with a single x-ray energy spectrum. In the diagnostic energy range, x-ray energy-dependent attenuation can be approximated as a linear combination of photoelectric absorption and Compton scattering. Hence, two physical components of x-ray attenuation can be determined from two spectrally informative projection datasets to achieve monochromatic imaging and material decomposition. In this paper, a projection-domain image reconstruction method is proposed to accurately quantify the two attenuation components for dual-energy CT. This method combines both an analytical algorithm and a single-variable optimization method to solve the non-linear polychromatic x-ray integral model, allowing an efficient and accurate decomposition of physical basis components. Numerical tests are performed to illustrate the merit of the proposed method.

Keywords—Dual-energy CT, polychromatic physical model, monochromatic image reconstruction, material decomposition.

I. INTRODUCTION

COMPUTED tomography (CT) can reconstruct a three-dimensional image of an object from a series of projections, providing important diagnosis information. In clinical CT, an x-ray source is polychromatic, and x-ray detectors are currently operated in a current-integrating mode. CT image reconstruction is based on an approximate line integral model, ignoring x-ray energy information. However, lower energy photons are more easily absorbed than higher energy photons, which would cause the x-ray beam to become increasingly harder as it propagates through the object [1]. This physical model mismatch would generate significant beam-hardening artifacts in the reconstructed image. Dual-energy CT is a well-established technique, allowing monochromatic imaging and material decomposition [2, 3]. Current dual-energy x-ray imaging methods include kVp-switching, dual-layer detection, dual-source scanning, and simplistic two-pass scanning.

This work was supported by the National Institutes of Health Grant NIH/NIBIB R01 EB016977 and U01 EB017140.

W. Cong D. Harrison, and G. Wang are with the Biomedical Imaging Center, Department of Biomedical Engineering, Rensselaer Polytechnic Institute, Troy, NY 12180 USA (cong@rpi.edu, danharrison@nycap.rr.com, wangg6@rpi.edu).

Y. Xi is with First Imaging Technology, Shanghai 201318, China (xiyansitu@gmail.com).

Several image reconstruction methods for dual-energy CT were developed over the years. Alvarez and Macovski proposed an image reconstruction method in the projection domain by solving a non-linear integral equation to decompose dual-energy measurements into two independent sinograms, each of which corresponds to a basis component [2]. Alternatively, image-domain reconstruction methods first reconstruct images from the low- and high-energy sinograms using filtered back projection (FBP), and then perform image-domain material decomposition [4, 5]. This type of image-domain reconstruction makes substantial approximations in energy spectra, resulting in quantitatively inaccurate results [6]. Recently, statistical iterative methods incorporate an accurate physical model to reconstruct images directly from dual-energy measurements [7]. These approaches involve a highly nonlinear forward model in the maximum likelihood framework to model the polychromatic measurement, representing a complicated nonlinear optimization problem. The great computation cost and slow convergence speed significantly reduces the practicality of the algorithm.

In this paper, a new image reconstruction approach for dual-energy CT is proposed based on a realistic polychromatic physical model. This method combines an analytical algorithm and a single-variable optimization method to solve the non-linear polychromatic x-ray integral model in the projection domain, allowing an efficient and accurate decomposition for sinograms of two physical basis components. In the next section, the physical model and reconstruction methods are described. In the third section, representative numerical experiments are presented. In the last section, relevant issues are discussed.

II. METHODOLOGY

A CT x-ray source generally emits a polychromatic spectrum of x-ray photons, and the x-ray linear attenuation through the object depends on the object material composition and the photon energy. After a polychromatic x-ray beam passes through the object, the x-ray intensity I measured by a current-integrating detector can be described by the non-linear integral model [2]:

$$I = \int_{E_{\min}}^{E_{\max}} S(E) \exp\left(-\int_l \mu(r, E) dr\right) dE, \quad (1)$$

where $S(E)$ is the energy distribution (spectrum) of the x-ray source, and $\mu(r, E)$ is the linear attenuation coefficient at an energy E and a spatial position r along an linear path l through the object. During propagation through the object, the x-ray photons population is statistically attenuated according to the nonlinear equation (1).

It is well known [2, 8] that photoelectric absorption and Compton scattering are the two dominant x-ray attenuation processes in the 20 keV-140 keV diagnostic energy range. The resulting x-ray linear attenuation coefficient can be represented by [2, 8, 9]:

$$\mu(r, E) = \rho \frac{N_A}{A} (\sigma_{ph} + \sigma_{co}), \quad (2)$$

where ρ , N_A , and A are mass density, Avogadro's number (6.022×10^{23} atom/g-atom) and atomic mass respectively. The photoelectric atomic cross section, σ_{ph} , is formulated as [10]

$$Z^4 \alpha^4 \frac{8}{3} \pi r_e^2 \sqrt{\frac{32}{\varepsilon^7}} \text{ for } \varepsilon < 1, \quad (2a)$$

where $\varepsilon = E/511$ keV, Z is the atomic number, α is the fine-structure constant ($\approx 1/137$), and $r_e = 2.818$ fm is the classical radius of an electron. The Compton atomic cross section, σ_{co} , is formulated as $Z f_{kn}$, where f_{kn} is the Klein-Nishina function:

$$f_{kn}(\varepsilon) = 2\pi r_e^2 \left(\frac{1+\varepsilon}{\varepsilon^2} \left[\frac{2(1+\varepsilon)}{1+2\varepsilon} - \frac{1}{\varepsilon} \ln(1+2\varepsilon) \right] + \frac{1}{2\varepsilon} \ln(1+2\varepsilon) - \frac{1+3\varepsilon}{(1+2\varepsilon)^2} \right) \quad (2b)$$

With both photoelectric and Compton atomic cross sections, the associated linear attenuation coefficients can be expressed as the product of spatial-dependent and energy-dependent components:

$$\mu(r, \varepsilon) = a(r)p(\varepsilon) + c(r)q(\varepsilon), \quad (3)$$

where

$$a(r) = \rho Z^4 / A \quad (3a)$$

is the spatial-dependent photoelectric component,

$$c(r) = \rho Z / A \quad (3b)$$

is the spatial-dependent Compton scattering component,

$$p(\varepsilon) = N_A \alpha^4 \frac{8}{3} \pi r_e^2 \sqrt{\frac{32}{\varepsilon^7}} \quad (3c)$$

is the energy-dependent photoelectric component, and

$$q(\varepsilon) = N_A f_{kn}(\varepsilon) \quad (3d)$$

is the energy-dependent Compton scattering component.

With dual energy CT, we have two distinct spectral measurements associated with each projection angle. Inserting

Eqs. (3) into Eq. (1) and using the first x-ray energy spectral measurement, we have

$$\begin{aligned} I_1 &= \int_{\varepsilon_{\min}}^{\varepsilon_{\max}} S_1(\varepsilon) \exp\left(-p(\varepsilon) \int_l a(r) dr - q(\varepsilon) \int_l c(r) dr\right) d\varepsilon \\ &= \int_{\varepsilon_{\min}}^{\varepsilon_{\max}} S_1(\varepsilon) \exp\left(-p(\varepsilon) \int_l a(r) dr - q(\varepsilon) \int_l \bar{c}(r) dr\right) \\ &\quad \times \exp\left(-q(\varepsilon) \int_l [c(r) - \bar{c}(r)] dr\right) d\varepsilon \end{aligned} \quad (4)$$

where $\bar{c}(r)$ is an initial estimation of the spatial-dependent Compton scattering component $c(r)$. For example, the mass density, atomic mass and the atomic number of water may be applied for the estimation of $c(r)$. The use of the initial estimation $\bar{c}(r)$ can effectively enhance the accuracy of a low-order Taylor expansion that is applied to the second exponential term in Eq. (4). Applying a fourth-order Taylor expansion, we have

$$\begin{aligned} I_1 &= \int_{\varepsilon_{\min}}^{\varepsilon_{\max}} S_1(\varepsilon) \exp\left(-p(\varepsilon) \int_l a(r) dr - q(\varepsilon) \int_l \bar{c}(r) dr\right) \\ &\quad \times \left[1 - q(\varepsilon)x + \frac{1}{2}q^2(\varepsilon)x^2 - \frac{1}{6}q^3(\varepsilon)x^3 + \frac{1}{24}q^4(\varepsilon)x^4 \right] d\varepsilon \quad (5) \\ &= \left[p_0(y) + p_1(y)x + p_2(y)x^2 + p_3(y)x^3 + p_4(y)x^4 \right], \\ &\quad x = \int_l [c(r) - \bar{c}(r)] dr, \quad y = \int_l a(r) dr. \end{aligned}$$

Eq. (5) is a quartic equation, and there are analytic solutions. It is easy to know that the polynomial function with respect to the variable x is strictly convex, typically yielding two real roots and a pair of conjugate complex roots. Generally, we can obtain the true solution, denoted as $x = h(y)$, from the prior range of the x value. Also, applying the second spectral measurement, the projection of the spatial-dependent photoelectric absorption distribution can be computed from the following single variable optimization,

$$y_{\min} = \arg \min \left\| I_2 - \int_{\varepsilon_{\min}}^{\varepsilon_{\max}} S_2(\varepsilon) \exp[-p(\varepsilon)y - q(\varepsilon)h(y)] d\varepsilon \right\|. \quad (6)$$

Eq. (6) can be effectively solved via single variable optimization, such as golden section search and parabolic interpolation. Therefore, the projections of spatial-dependent photoelectric absorption and Compton scattering images can be effectively determined by solving Eqs. (5) and (6) simultaneously for every detector elements at each projection view.

III. NUMERICAL EXPERIMENTS

In the numerical simulation, the x-ray imaging process was simulated with an x-ray tube operated at 120 kVp/200mA. Two x-ray energy spectra can be generated from the x-ray tube at a single kVp setting by using the Grating Oriented Line-wise Filtration technique [11]. The GOLF technique is a

combination of absorption and filter gratings (placed between the source and

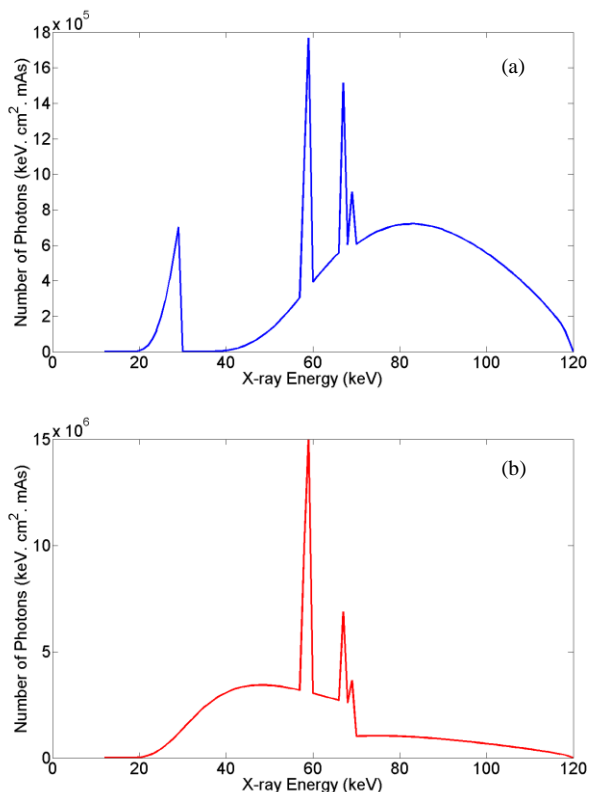


Fig. 1. Energy spectral distributions of the x-ray source simulated using the public software SpekCalc [12]. (a) The energy spectrum generated from the x-ray tube (120 kvp) filtered by Tin of 0.5mm thickness, and (b) the energy spectrum from the x-ray tube (120 kvp) filtered by Tungsten of 0.05mm thickness.

patient/object) that are driven in relative motion that is synchronized with detector view acquisition. Using micro-technology to fabricate the gratings, the medical CT requirements for a large field of view, large cone angle, and rapid change between filtration settings can be simultaneously met.

Tissue	1	2	3	4	5	6	7	8	9
Z	3.04	4.90	4.02	5.15	5.09	4.58	5.91	5.39	5.64
ρ	1.00	0.96	0.99	1.07	1.06	1.03	1.20	1.06	1.10
A	6.49	8.93	7.35	8.90	9.34	13.96	8.22	10.12	9.32

Single-slice CT imaging was assumed and used a parallel beam geometry. The source-to-iso-center distance was set to 54.1 cm and the source-to-detector distance was set to 94.9 cm. A Shepp-Logan-type phantom was designed to contain 9 sub-regions that were filled with various human tissues. The effective atomic numbers, densities, and atomic masses in these sub-regions, which characterized photoelectric and Compton cross-sections, are listed in Table 1. The phantom diameter was

set at 440 mm and the phantom was placed at iso-center. The phantom was discretized into 512×512 square pixels.

Then, energy-dependent linear attenuation coefficients were synthesized according to Eq. (3). The projection datasets were generated for 180 views over a range of 180° based on Eq. (1) and using the two energy spectra shown in Fig. 1. By interpolation methods, low-energy data and high-energy data were well aligned at each projection view. The projection data were corrupted by Poisson noise to simulate real experiments.

The proposed algorithm was applied for reconstruction of the photoelectric-absorption and Compton-scattering images from the two projection datasets. The reconstructed spatial-dependent photoelectric absorption and Compton scattering images are in excellent agreement with the truth, the detailed features are quantitatively accurate, and beam hardening effect is basically overcome, as shown in Figs. 2-3. Hence, the attenuation coefficient at each energy bin can be computed based on Eq. (3) to achieve a monochromatic image reconstruction. For comparison, we also performed the attenuation image reconstruction based on the line integral model. Because of the beam hardening effect, it is observed that the reconstructed image with the line integral model contains cupping artifacts, as shown in Fig. 4.

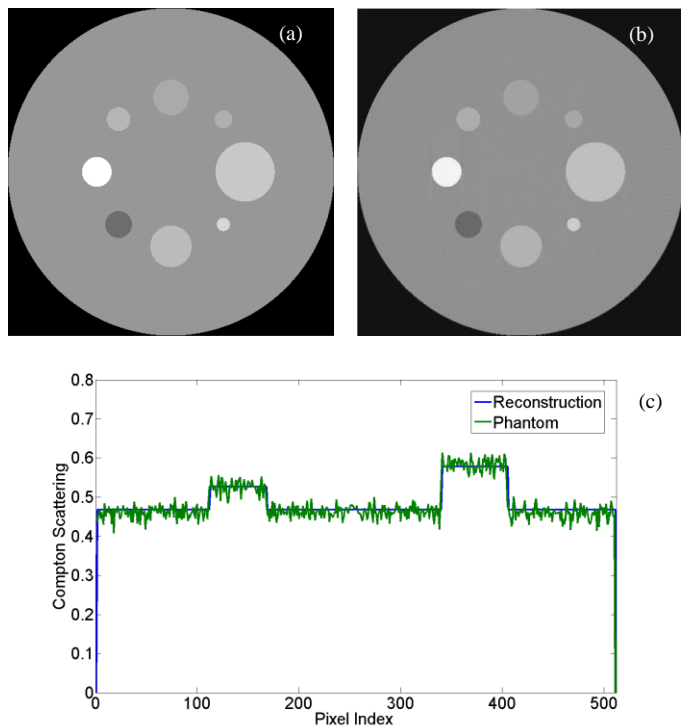


Fig. 2. Image reconstructions of the numerical phantom. (a) The true Compton scattering image, and (b) the reconstructed Compton scattering image, and (c) the profiles along the vertical midlines in the phantom and reconstructed images.

IV. CONCLUSION

An image reconstruction method has been proposed to accurately decompose components in the physical basis for dual-energy CT, from which the monochromatic image reconstruction can be obtained. This method combines an

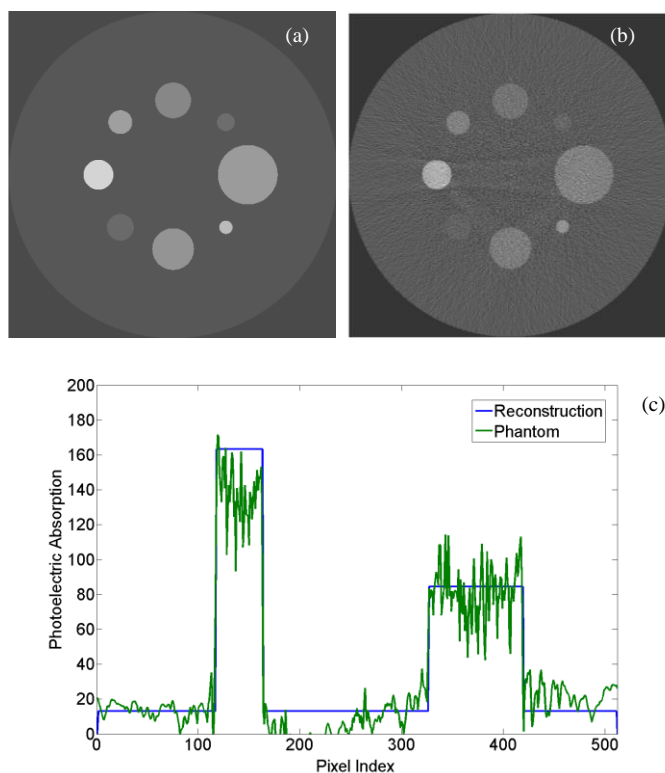


Fig. 3. Image reconstructions of the numerical phantom. (a) The true photoelectric absorption image, and (b) the reconstructed photoelectric absorption image, and (c) the profiles along the horizontal midlines in the phantom and reconstructed images.

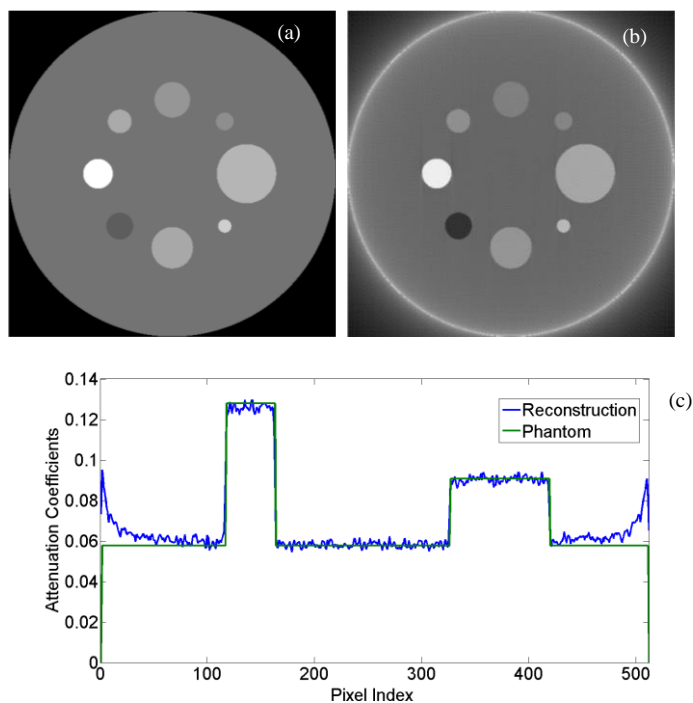


Fig. 4. Image reconstructions of the numerical phantom. (a) The average attenuation coefficient image from the phantom, (b) the reconstructed attenuation image based on the linear integral model, and (c) profiles along the vertical midlines in the phantom and reconstructed images.

analytical algorithm and a single-variable optimization method to solve the non-linear polychromatic x-ray integral model, allowing an efficient and accurate decomposition for sinograms of two physical basis components, and avoiding the beam hardening issue associated with the image reconstruction in conventional CT based on the linear integral model. Numerical results have been analyzed to illustrate the merit of the proposed image reconstruction method. We are seeking real datasets to further evaluate the image quality in clinical applications. The proposed method is applicable to biomedical imaging, nondestructive testing, food inspection, and security screening.

REFERENCES

- [1] B. De Man, J. Nuyts, P. Dupont, G. Marchal, and P. Suetens, "An iterative maximum-likelihood polychromatic algorithm for CT," *IEEE Transactions on Medical Imaging*, vol. 20, no. 10, pp. 999-1008, Oct, 2001.
- [2] R. E. Alvarez, and A. Macovski, "Energy-Selective Reconstructions in X-Ray Computerized Tomography," *Physics in Medicine and Biology*, vol. 21, no. 5, pp. 733-744, 1976.
- [3] L. Yu, S. Leng, and C. H. McCollough, "Dual-energy CT-based monochromatic imaging," *AJR Am J Roentgenol*, vol. 199, no. 5 Suppl, pp. S9-S15, Nov, 2012.
- [4] T. Niu, X. Dong, M. Petrongolo, and L. Zhu, "Iterative image-domain decomposition for dual-energy CT," *Med Phys*, vol. 41, no. 4, pp. 041901, Apr, 2014.
- [5] T. P. Szczykutowicz, and G. H. Chen, "Dual energy CT using slow kVp switching acquisition and prior image constrained compressed sensing," *Phys Med Biol*, vol. 55, no. 21, pp. 6411-29, Nov 07, 2010.
- [6] C. Maass, M. Baer, and M. Kachelriess, "Image-based dual energy CT using optimized pre-correction functions: a practical new approach of material decomposition in image domain," *Med Phys*, vol. 36, no. 8, pp. 3818-29, Aug, 2009.
- [7] R. Zhang, J. B. Thibault, C. A. Bouman, K. D. Sauer, and J. Hsieh, "Model-Based Iterative Reconstruction for Dual-Energy X-Ray CT Using a Joint Quadratic Likelihood Model," *IEEE Trans Med Imaging*, vol. 33, no. 1, pp. 117-34, Jan, 2014.
- [8] E. B. Podgoršak, *Radiation physics for medical physicists*, 2nd, enl. ed., Heidelberg: Springer, 2010.
- [9] Z. H. Qi, J. Zambelli, N. Bevins, and G. H. Chen, "Quantitative imaging of electron density and effective atomic number using phase contrast CT," *Physics in Medicine and Biology*, vol. 55, no. 9, pp. 2669-2677, May 7, 2010.
- [10] E. B. Podgorsak, *Radiation Physics for Medical Physicists*, Heidelberg: Springer, 2010.
- [11] Y. Xi, W. Cong, D. Harrison, and G. Wang, "Grating Oriented Line-wise Filtration (GOLF) for Dual-energy X-ray CT," *Phys Med Biol*, under review, 2016.
- [12] G. Poludniowski, G. Landry, F. DeBlois, P. M. Evans, and F. Verhaegen, "SpekCalc: a program to calculate photon spectra from tungsten anode x-ray tubes," *Phys Med Biol*, vol. 54, no. 19, pp. N433-8, Oct 07, 2009.